ХИМИЧЕСКАЯ ФИЗИКА, 2004, том 23, № 9, с. 3–7

ГОРЕНИЕ И ВЗРЫВ

УДК 541.126

PLASMA-SURFACE INTERACTIONS FOR LANGMUIR PROBE IMMERSED IN HYDROCARBON COMBUSTION FRONT

© 2004 A. Cenian[1, *], A. Chernukho[2], A. Bogaerts[3], C. Leys[4]

[1]*Institute of Fluid-Flow Machinery, Polish Academy of Sciences, 80-952 Gdansk, Fiszera 14, Poland*

[2]*Heat and Mass Transfer Institute, P.Brovki Street 15, 220072 Minsk, Belarus*

[3]*Department of Chemistry, University of Antwerp, Universiteitsplein 1, B-2610 Antwerp-Wilrijk, Belgium*

[4]*Department of Applied Physics, Ghent University, B-9000 Gent, Rozier 44, Belgium*

Received 01.10.2003

Langmuir-probes immersed in a combustion front are effective tools of flame-plasma diagnostics, including determination of flame-front arrival, ion temperature or ionization density. Particle-in-cell Monte-Carlo models, combined with computational fluid-dynamics and ion-kinetics codes may be very helpful in providing some additional information useful in interpretation of probe data. The results of the first particle-in-cell simulation of current-voltage characteristic of Langmuir probe are presented here.

1. INTRODUCTION

Langmuir probe is a well-established diagnostic tool of a low pressure, stationary plasma [1]. It allows determining the electron and ion densities, temperatures, *etc*. Moreover, a procedure of charge currier identification was discussed *e.g*. by Studniarz [2]. The electrical probe was already applied as an indicator of combustion-front arrival [3–5]; however, serious problems arise when more detailed characteristics of "combustion" plasma *i.e*. high-pressure, non-stationary, multi-ion medium, are investigated. Series of experiments on electric-probe diagnostics of combustion plasma were performed by MacLatchy *et al*. (see *e.g*. [6–8]) and Hirano et al. (*e.g*. [9, 10]). Lately Labuda et al. have done some experiments for probe immersed in combustion front propagating through a closed vessel – see *e.g*. [11].

The standard models of Langmuir probe (see *e.g*. [1]) as well as the Bohm criterion of sheath formation [12, 13] cannot be straightforward applied [14]. The realistic probe models (based *e.g*. on Fluid or Particle-in-cell approach) should take into account plasma-probe interactions in a multi-collisional sheath. The **Fluid Models** are based on a solution of the Boltzmann (or its moments i.e. continuity, momentum and energy conservation-equations) and Poisson equations. In the **Particle-In-Cell Monte-Carlo** (PIC-MC) models the Boltzmann equation and the averaging procedure using a derived EEDF, are substituted by a numerical integration of an observable along the "quasi-particle" trajectories. Each "quasi-particle" represents large number ($\sim 10^5$–10^{10}) of electrons, positive and negative ions moving in the electric field determined by a solution of Poisson's equation. A simulation box is divided by computational grid, with spacing $(1/4)\lambda_D$ often assumed. The number of grids points considered varies between few hundreds and few thousands (*e.g*. 200 [15] or 2560 [16]). The particles crossing the simulation box boundaries are removed (or specular-reflected), whereas the particles injected at the boundaries are added to the simulations. The collisions are treated by MC methods as instantaneous processes, governed by the probability law related to the measured cross sections. Some ous approximations are applied, in order to make the problem computationally treatable.

The plasma-wall interactions have lately been investigated by using various PIC-MC models, *e.g*. [15, 17, 18]. For example, an important fundamental issue of multiple-sheath formation in electronegative discharges was discussed.

Kono [15] has proposed **the spherical 1d2v** (1*D* displacement 2*D* velocity) **PIC-MC model** for the probe immersed in the plasma. It determines the MC trajectories of all charged particles (including electrons), which gradually fills the empty simulation box due to the thermal particle flux from ambient plasma. The particles passing the boundaries of the simulation box are lost (absorbed on the wall or into ambient plasma). All particles move in the determined electric field. The ion collisions are treated in a simplified manner *i.e*. the velocity of the colliding particle is replaced by the random thermal velocity corresponding to the temperature of that species and $T^+ = T^- = T_e/100$ is assumed. The stationary particle-density and potential profiles are determined.

The **1d3v** (1*D* displacement 3*D* velocity) **PIC-MC model** for electropositive plasma systems of cylindrical geometry was proposed by Kawamura et al. [18]. The 3*D* trajectories are calculated, however, only radial (1*D*) dependence of charge distribution is taken into account in Poisson's equation (due to radial symmetry). The axial component of charged particle velocity, introduced to the model, enables determination of self-

*Corresponding author – e-mail: cenian@imp.gda.pl

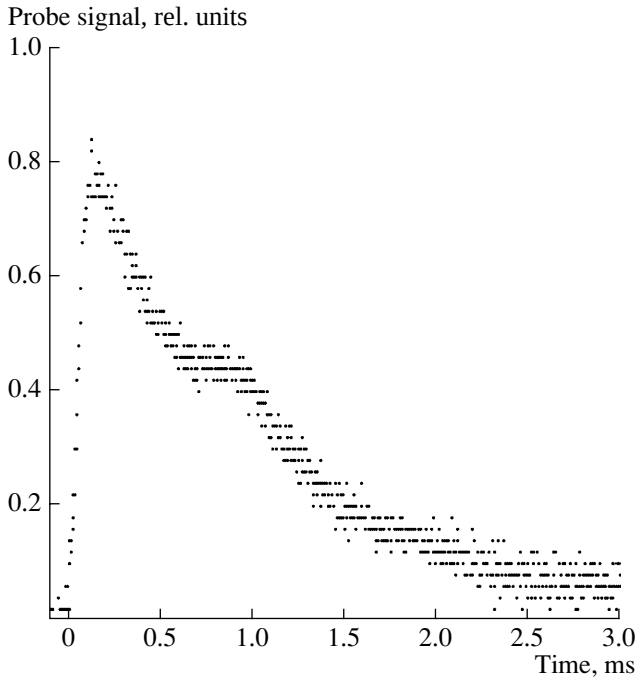

Fig. 1. Langmuir probe signal in propane-butane/air stoichiometric mixture flame.

sustained electric field corresponding to the chosen current density. The assumption about the charge loss and gain balance is used here i.e. at steady state electron ionization processes should balance electron losses (in volume and at the wall). The gas temperature (T), gas density (N_g), discharge tube radius (R) and axial currents are treated as the initial parameters. The rest including axial field (E_z), spatial and velocity distribution of electrons and ions are calculated from the first principles, assuming $E_z(r)$ = const. The initial distribution of charged particles is spatially uniform, while velocities are determined using fixed energy (for electrons) or Maxwellian distribution (for ions). Already introductory investigations [14] proved that this model could be useful to study fundamental problems of plasma-wall interaction, including plasma neutrality, Bohm criterion and sheath formation.

Both, the process of sheath generation and sheath structure depend on ion identities and concentrations. It is generally accepted that the primary ion in hydrocarbon flames (CHO^+) is produced during the well-known Calcote mechanism [19]. However, there are some fast charge transfer and electron attachment processes, which lead soon to appearance of great variety of other ions. And so, Egsgaard and Carlsen [20] have found (using mass-spectroscopy) that H_3O^+ and $C_3H_3^+$ ions prevail during combustion of CH_4, C_3H_8, CH_4/C_2H_4 and CH_4/C_2H_2 mixtures with oxygen. Fialkov [21] has reported, however, that the second ion plays major role only in fuel-rich flames.

Among the negatively charged species, produced in stoichiometric, low pressure methane flames, OH^- and CH_3^- ions prevail according to Feugier and van Tiggelen [22], but HCO_2^-, CO_3^-, $C_2H_3O^-$, OH^-, C_6H^- and C_2H^- were found by Sugden et al. (1976) [23] in fuel-rich flames, with O_2^- as the primary negative ion.

The presence of nitrogen (air) in the combustion chamber significantly influences ion composition – see *e.g.* [24–26]. In that case, NO^+, NH_4^+, NCO^-, CN^- and CN_2^- ions play major role. Finally, Starik and Titova [27] have found from simulations of hydrocarbon/air combustion, that the main ion species, which should be taken into account to simulate the real combustion plasma, are NO^+, H_3O^+, $C_2H_3O^+$, NO_3^-, NO_2^- and CO_3^-.

2. TIME EVOLUTION OF LANGMUIR-PROBE SIGNAL

Figure 1 presents the time evolution of a current signal for the spherical probe (r_p = 0.1 mm, positively polarized) immersed in a combustion front propagating in stoichiometric LPG(propane-butane)/air mixture [28]. The signal rise-time lies in the range 0.12–0.2 ms. A double structure observed indicates that at least two negatively-charged species take part in the process of sheath formation. Taking into account, a significant decrease of the probe-current after changing voltage polarization, one might conclude that one of these negatively charged species are electrons.

The decay time of the first peak – related to the "electron" current – is smaller than 0.55 ms. This corresponds fairly well with the combustion-front thickness. As the chemi-ionization (and electron formation) takes place mainly in the combustion front (see *e.g.* [21]) it supports the idea that the first peak is related to the electron current. The following plateau and the second decay time (~1.4 ms) of the current signal are determined by the negative ion kinetics (probably by the recombination of NO_3^- [27]).

3. MODELING OF PLASMA-SURFACE INTERACTION

The modeling of combustion-plasma and probe interactions should include considerations related to the gasdynamic flows, chemical kinetics and plasma-dynamics. Here we investigate only the last stage i.e. the plasma-dynamic. The results of simulations will be later included into general combustion model. The 1d3v PIC-MC model (related to these of Kono [15], Kawamura et al. [18] and Cenian et al. [14]) will be used in order to check the possibility to derive probe characteristic. Because of model complexity and lack of data relative to the ions listed above, only 1-ion approximation

will be used at this stage. The (positive) ion will be described by the mass to charge (m/z) ratio and the set of cross sections described in [14, 29, 30].

The plasma-probe interactions are studied in the system with the radial symmetry (related to the infinitely long cylindrical probe, $2r_p$ in diameter, immersed in a continuum, non-flowing, electro-positive plasma – see Fig. 2). The whole space is separated (for the sake of simplification) into three different zones: Sheath-Pre-Sheath (SPS) zone, ring-shaped volume around it (called later "buffer zone") and the infinite rest (equilibrium "bulk plasma"), which serve as a particle-source or particle–sink for the buffer zone. The MC trajectories are calculated only for the charged particles present in SPS and buffer zones. The neutral plasma outside the pre-sheath is described by the electron (T_e) and ion (T_i) temperatures. There is a continuous exchange of particles between all zones; however, the charged particle concentration in the buffer zone is kept constant, by supplying a new particle from, or by a particle-loss to the bulk plasma. The charged particle concentration in the buffer is determined from the assumed gas pressure and ionization degree ($\alpha = N_i/N$).

Initially the SPS zone is free of charged particles. However, there is a continuous thermal flux of ions and electrons, which brings the charged species from the buffer zone to the pre-sheath zone. As soon as the charged particle enter the pre-sheath region an additional particle is supplied to the buffer from the bulk plasma in (r_b) with the same velocity; here $2r_b$ is outer diameter of the buffer zone. When, a charged particle is lost to the bulk in phase-space point (r, v_r, v_t), another one enters the bulk-buffer border in (r, $-v_r$, v_t).

The charged-particle trajectories are governed by Newtonian equations taking into account the field generated by the probe as well as that related to the charged particle density (through the Poisson equation). It is assumed that the electric field vanishes, $E = 0$, at the pre-sheath edge. The probe surface is assumed to be fully absorptive (both for electrons and ions) i.e. a particle is removed from simulation when its trajectory passes the probe wall ($r < r_p$). The difference between numbers of absorbed electrons and ions determines the probe current. The various speeding up methods of PIC-MC code were used – see *e.g.* [18], including: subcycling, improved initial density profile, light ions, variable particle weights and constraints on time and space-step.

4. RESULTS AND DISCUSSION

The following values of the model parameters were used here:

gas density $N = 10^{24}$ m^{-3},

ionization degree $\alpha = 10^{-7}$,

ion kinetic energy $T_i = 3000$ K,

electron kinetic energy $T_e = 0.5$ eV,

ion mass to its charge ratio $m/z = 19$,

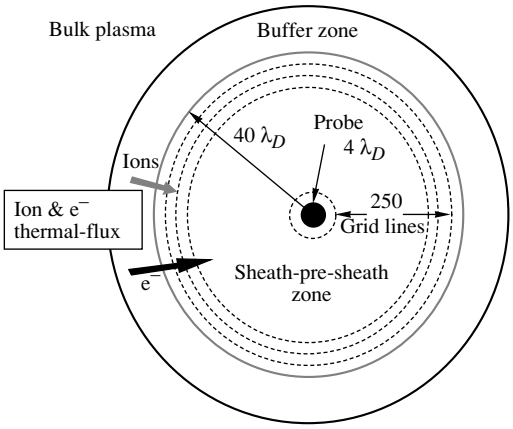

Fig. 2. Scheme of the probe-model including bulk plasma, buffer and sheath-pre-sheath zones; electron and ions temperatures are 0.5 eV and 3000 K, respectively.

Debye length $\lambda_D = 1.2 \cdot 10^{-5}$ m,

probe radius $r_p = 4\lambda_D$,

SPS zone radius $r_s = 44\lambda_D$,

outer-diameter of buffer zone $D_b = 2r_b = 93\lambda_D$.

It should be stressed here that ionization degrees exceeding $\alpha = 10^{-7}$ were found *e.g.* in simulation [27], at least at the combustion front. The applied m/z value corresponds to H_3O^+ i.e. one of the main ions in the combustion front. It should be stressed that the simulation presented here is limited by the knowledge of the CS for electron and ion processes.

Figure 3 presents profiles of potential generated in sheath-pre-sheath zone for different bias voltages of the probe, $-50 < V_p < 30$ V, the last determined relative to the bulk plasma. The potential was derived from the integral form of Poisson equation, basing on the number of charged particles accumulated in 250 grid cells of the SPS zone – see Fig. 4. The smooth transition of the calculated potential-profiles to the border condition – $\partial V/\partial r(44\lambda_D) = 0$, testifies that the simulation zones are chosen properly. The effective diameter of a pre-sheath zone (given by position where the electric field practically vanishes, $E \sim 0$) increases with the probe bias-voltage.

The presented in Fig. 4 ion-density profiles are quite erratic (especially at low probe potentials) due to small ion mobility. A significant increase of ion densities in the sheath region (close to the probe surface) absent in the case of our previous simulations [14] should probably be related to the change of geometry. In Ref. [14], the ion-flux to the tube wall was divergent, in contrast to the converging flow to the investigated probe. The importance of geometry for plasma-dynamics was already pointed out by Kono [15]. A significant drop of both electron and ion densities in the volume around the probe should be stressed.

Figure 5 shows a probe characteristic – with an inclusion presenting details of its ionic part. The very

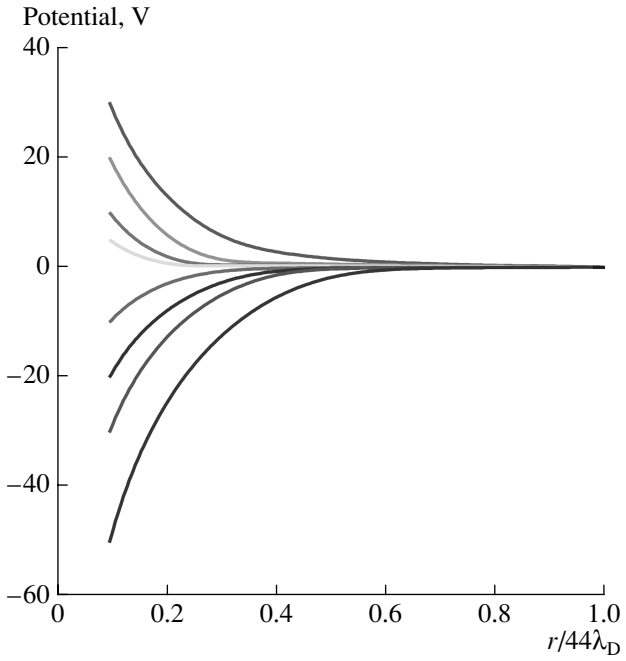

Fig. 3. Spatial profiles of the plasma potential for probe bias voltage, $-50 < U_b < 30$ V.

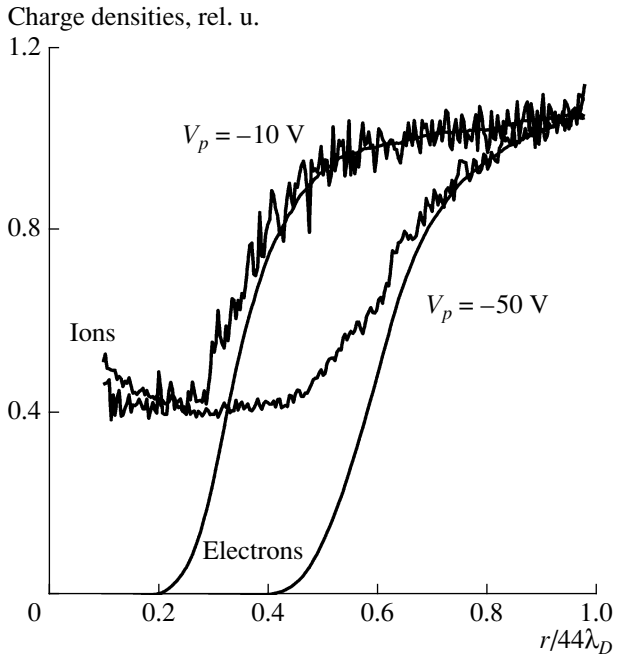

Fig. 4. Electron- and ion-density profiles for probe-bias voltages –10 and –50 V.

large difference between the ionic and electronic currents is related both: to the ion/electron mass (mobility) as well as to the assumed ratio $T_i/T_e \sim 0.52$. The applied T_i/T_e value does not differ significantly from the one estimated by Calcote [19] for a low-pressure acetylene/oxygen flame but it is significantly larger than that related to a propane/air mixture at high-pressure ($T_i/T_e \sim 0.8$). Moreover, the combustion-plasma is generally strongly electro-negative i.e. $n_e/n_i \ll 1$ [14, 19, 27], in contrast to the one considered here. The electron-attachment processes can significantly reduce the electron current to the probe. This effect cannot be, however, discussed in frame of the 1-ion approximation used here and must be postponed to future simulations.

The saturation currents are limited by the charged-particles thermal-flux to the STS zone. In the case presented here, the electron thermal-flux per unit length of the probe at the STS outer-border ($r_s = 44\lambda_D$) was estimated to be 9 mA/mm, while the electron current determined for $V_p = 20$ V is ~ 1 mA/mm. Positive ion flux at the same border was 30 μA/mm i.e. more than 2 orders of magnitude less than electron thermal flux.

The floating potential, estimated from the characteristic, is equal 2.2 V. This could be compared with the values 2.15 and 2.5 V derived from the formulas given by Lieberman and Lichtenberg [31]

$$V_f = -T_e/2[\ln(M/2\pi m_e)]$$

or Raiser [32]

$$V_f = -T_e[1 + 1/2\ln(M/4\pi m_e)],$$

for a low pressure plasma.

The electron temperature can also be determined from a slope of the characteristic, when current is presented in the logarithmic scale. The well-known relation

$$I = I_0 \exp(eV_p/kT_e),$$

where I is the current value at the potential V_p, gives $T_e = 0.55$ eV for the voltage region between the floating

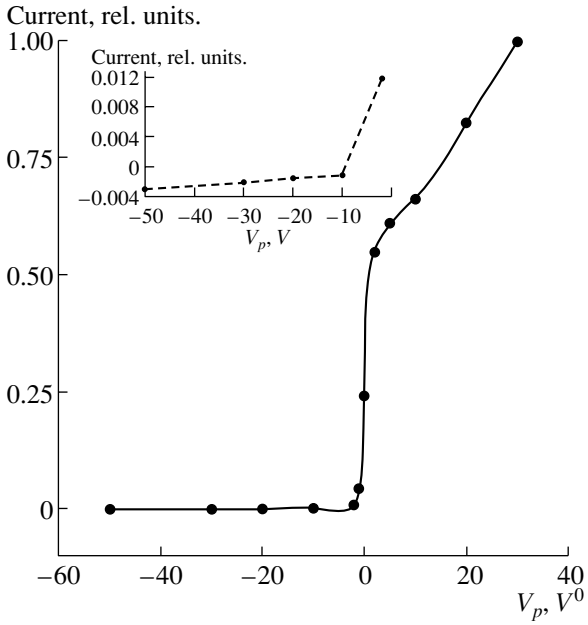

Fig. 5. Voltage-current characteristic of probe.

and plasma potentials. This is very close to the assumed T_e value, what confirms the applied numerical procedure.

5. CONCLUSIONS

Langmuir-probes immersed in a combustion front are effective tools of flame-plasma diagnostics. They enable determination of flame temperature, ionization density, arrival of combustion front, *etc*. In order to get more information about the plasma characteristics one should know the details of plasma kinetics in the combustion front. Particle-in-cell Monte-Carlo models, combined with computational fluid-dynamics and ion-kinetics codes can be very helpful in providing some additional information.

It should be stressed that according to our knowledge, the presented here results describe the first attempt to simulate a probe characteristic using PIC MC model. Therefore, the considered simplifications of plasma model could be accepted at this stage. The future models should include plasma kinetics of hydrocarbon flames and available cross sections for main plasma-chemical constituents of hydrocarbon flames. Additional information about relation between electron and ion temperatures in the combustion front is desirable.

It is worth to note that the simulated characteristic enables the correct determination of electron temperature assumed in the model. So, the numerical procedures applied here have been positively confirmed.

ACKNOWLEDGMENTS

We acknowledge financial support from the bilateral Belgium – Polish cooperation program and the Project 4T10B 01922 of Polish Committee for Scientific Researches.

REFERENCES

1. *Mott-Smith H.M., Langmuir I.* // Phys. Rev. 1926. V. 28. P. 727.
2. *Studniarz S.A.* // Electrical discharges, in Ion Molecular Reactions/Ed. Franklin J.L., Butterworth, London, 1972. P. 647.
3. *Conzelmann G., Knapp H.* // MTZ Motortechnische Zeitschrift. 1961. V. 22. P. 9.
4. *Wenzlawski K., Heintzen D.* // MTZ Motortechnische Zeitschrift. 1990. V. 51. P. 118.
5. *Bellenoue M., Cenian A., Kageyama T., Labuda S.A., Leys C.* // Twenty-Ninth Int. Symp. on Combustion. Sapporo, Japan. Abstracts of W-I-P, 2002. P. 126.
6. *MacLatchy C.S.* // Combust. and Flame 1979. V. 36. P. 171.
7. *MacLatchy C.S.* // IEEE Transactions on Plasma Sci. 1989. V. 17. P. 29.
8. *MacLatchy C.S., Smith H.C.L.* // IEEE Trans. Plasma Sci. 1991. V. 19. P. 1254.
9. *Hirano T.* // Trans. JSME. 1972. V. 37. P. 1204.
10. *Hirano T. et al*. // Trans JSME. 1980. V. 46. P. 1007.
11. *Cenian A., Labuda S.A., Leys C., Bellenoue M.* // Combustion and Atmospheric Pollution / Ed. Roy G.D., Frolov S.M., Starik A.M. Moscow: TORUS PRESS Ltd, 2003. P. 115.
12. *Bohm D.* // The Characteristics of Electrical Discharges in Magnetic Fields / Ed. Gurthry A., Wakerling R.K., New York: MacGraw-Hill, 1949. P. 77
13. *Riemann K-U.* J. Phys D: Appl. Phys. 1991. V. 24. P. 493.
14. *Cenian A., Chernukho A., Leys C.* // Radiation Phys. and Chem. 2003. V. 68. P. 109.
15. *Kono A.* // J. Phys. D: Appl. Phys. 2001. V. 34. P. 1083.
16. *Sheridan T.E., Lonngren K.E.* // J. Appl. Phys. 1999. V. 86. P. 3530.
17. *Chabert P., Sheridan T.E.* // J. Appl. Phys. 2000. V. 33. P. 1854.
18. *Kawamura E., Ingold J.H.* // J. Phys. D: Appl. Phys. 2001. V. 34. P. 3150.
19. *Calcote H.F.* // Proc. 9-th Sym. on Combustion. New York: Academic Press, 1963. P. 622.
20. *Egsgaard H., Carlsen L.* // J. Anal. and Appl. Pyrolises. 1993. V. 25. P. 361.
21. *Fialkov A.B.* // Prog. Energy Combust. Sci. 1997. V. 23. P. 399.
22. *Feugier A., Van Tiggelen A.* // 10th Symp. on Combust. Pittsburgh: The Combust. Institute, 1965. P. 621.
23. *Goodings J.M., Bohme D.K., Sugden T.M.* Proc. 16th Sym. on Combust. Pittsburgh: The Combustion Institute, 1976. P. 891.
24. *Van Tiggelen A.* // Progress in Astronautics and Aeronautics. 1963. V.12. P. 165.
25. *Hayhurst A.N., Kittelson D.B.* // Combust. and Flame. 1978. V. 31. P. 37.
26. *Debrou G.D., Goodings J.M. et al.* // Combust and Flame. 1980. V. 39. P. 1.
27. *Starik A.M., N.S. Titova* // Combustion, Explosion, and Shock Waves. 2002. V. 38. P. 253.
28. *Cenian A., Chernukho A., Labuda S.A., Sawczak M., Leys C.* // Combustion and Atmospheric Pollution / ed. Roy G.D., Frolov S.M., Starik A.M., Moscow: TORUS PRESS Ltd., 2003. P. 109.
29. *Hegerberg R., Elford M.T., Skullerud H.R.* // J. Phys. B. 1982. V. 15. P. 797.
30. *Phelps A.V.* ftp://jila.colorado.edu/collision.data 1999.
31. *Lieberman M.A., Lichtenberg A.J.* Principles of plasma discharges and materials processing. N.Y.: Wiley-Interscience Publication, John Wiley & Sons, Inc., 1994.
32. *Raiser J.P.* Fizika gazovovo razriada. Moscow: Nauka, 1987.

SPELL: 1. specie, 2. radiusr, 3. ACKNOWLEDGEMENTS